

The effects of winds from burning structures on ground-fire propagation at the wildland–urban interface

Ronald G. Rehm^{1,*}

Guest Researcher and Retired NIST Fellow, National Institute of Standards and Technology, Gaithersburg, MD, USA

(Received 17 April 2007; final version received 21 November 2007)

A simple physics-based mathematical model is developed for prediction of the propagation of a grass-fire front driven by an ambient wind and by entrainment winds generated from one or more burning structures. This model accounts for the heterogeneous nature of the burning in a particular wildland–urban-interface (WUI) setting, where the entrainment from fundamentally three-dimensional structure-fire plumes can change the propagation of a two-dimensional ground-fire front. Data on grass fires and estimates of structure fires are presented and compared to justify the model. Scaling effects on the fire-front propagation-speed are given as a function of the location of the front, of the heat release rate of a single burning structure, of the total number of burning structures and of the burning-structure density. Also, detailed front propagation changes due to a single and multiple burning-house scenarios are presented.

Keywords: heterogeneous burning; mathematical model; outdoor fire spread; physics-based fire model; wildland–urban-interface fire model

1. Introduction

In 1997, Albini [1] presented an invited talk, entitled *An Overview of Research on Wildland Fire*, to members of the International Association for Fire Safety Science (IAFSS), who are mostly engineers and scientists concerned with fires in structures. Albini observed that while the interests of attendees ‘are focused mainly upon fire in man-made structures, many of its studies are relevant to, and applied in, modelling of wildland fire phenomenology. But the converse does not seem to be the case. Results of wildland fire research are seldom cited in the literature of fire safety research as it is done by this audience.’ In the process of communicating between the two groups, he observed that, ‘the learning burden in this process will probably be greater for wildfire specialists than for traditional fire safety science researchers . . . because the latter group strongly favors mathematical modelling of physical processes while wildland fire research traditionally incorporates a significant component of empiricism, often only weakly supported by conceptual models of underlying physical processes.’

Albini also noted that, ‘Interest by the general public in matters of wildland fire safety has grown with increased exposure of affluent society to the hazards posed by building flammable structures in flammable wildland settings.’ This quote is very important, I believe, because it

¹Current address: Building 224, Room B260 National Institute of Standards and Technology 100 Bureau Drive Gaithersburg, MD 20899, USA.

*Email: ronald.rehm@nist.gov and rehmro@comcast.net

explicitly acknowledges that structures, when ignited, become part of the fuel system. This statement challenges the notion that structures have little influence on fire behaviour which is held currently by land-management agencies. Since a structure is considered to be surrounded by wildland fuel and isolated from other structures, when a wildfire encounters the structure, it either resists the thermal insult, or it ignites. In either case according to this view, the structure is no longer of interest for determination of the wildfire behaviour. Albini's statement suggests rather that the fire behaviour with the structure included, will in general be different from the fire behaviour without the structure.

The objective of this paper is to develop a simple example of a physics-based model for wildland–urban-interface (WUI) fires which is useful without resorting to a complete Computational Fluid Dynamics (CFD) type of description of the phenomena. Another way of stating this objective is to ask the question, What would a generalization of the Rothermel model [2, 3] to WUI fires look like that was: (a) physics based, and (b) more complex and detailed, than the Rothermel model, but not as complex, mathematically and computationally, with the associated data requirements, as a CFD simulation? It is also hoped that this modelling effort might stimulate better communication and cooperation between wildfire specialists and fire safety scientists.

2. Physics-based models of fire behaviour

Fire spread in a heterogeneous-fuel environment, i.e. one having various types of fuels interspersed, is very complex and is not well understood. For example, at the WUI, both wildland fuels and structural fuels are found intermixed. Unfortunately, while discussed at length and used regularly as justification for additional research, little effort has been devoted to serious examination of the physical basis for WUI fire spread.

In the model proposed here, the fuel system will be regarded as having two components, the wildland-fuel or ground-fuel portion of the fuel system and the structural fuel component. Propagation of fires in the ground fuel portion, which is taken here to be grass, will be treated using an empirical relation to connect the fuel and wind to the rate of spread (ROS) of the fire, as it is in operational wildfire models, such as BehavePlus [4] and FARSITE [5]. Ignition between fuel types, i.e. grass to structure, structure to grass or structure to structure, envisioned in this model, takes place by direct flame impingement of the relatively small grass flames, by brands (or embers), which can either ignite structures directly, or start spot fires in the grass that can ignite structures ahead of the fire front (as illustrated in the detailed examples in the manuscript), or possibly by direct house-to-house fire spread.

In regions of significant topographical variation, the propagation of fires in ground fuels such as grasses, leaves or pine needles, or slash, etc. with an occasional tree or shrub, or even an occasional structure, can probably be predicted reasonably well by the methodology used in operational models. Furthermore, fires in large, nearly homogeneous tracts of trees in regions of significant topographical variation can also often be modelled reasonably well by these same procedures. When there are significant inhomogeneities in the fuel system, however, such as several structures, surrounded by grasses or other ground fuels, the limitations of the current operational methodology must be re-evaluated and new mathematical models must be considered for predicting fire behaviour.

Over the past several years, models of fire behaviour, based on the equations for conservation of mass, momentum, energy and species and for radiative transport, have been developed and applied very successfully, particularly to fires in structures. These so-called field models are based on a partial differential and integro-differential equations for the conservation laws. There are many examples of these field models, including the Fire Dynamics Simulator (FDS) [6, 7]; the

Wildland Fire Dynamics Simulator (WFDS) [8]; FIRETEC [9] and others. Colleagues in fire research at the National Institute of Standards and Technology (NIST) have been very active in the development of FDS and WFDS, together with their visualization code, Smokeview [10]. Therefore, because of my familiarity with these models and codes, when I discuss field models, I have FDS and WFDS in mind.

For a fully developed room-fire, the heat released by the fire generates a buoyant plume, which in turn entrains ambient room air, heats it and pumps it up into a hot, smoky upper layer. The room then becomes stratified into the ambient-air lower layer and the heated upper layer, with the fire continuing to remove air from the lower layer through entrainment and adding the heated air plus combustion products to the upper layer as time proceeds. As the fire grows, the whole room becomes involved in the fire, and the room is said to ‘flash over’. When this occurs, all of the contents of the room have been lost to the fire.

Usually, the fire does not remain confined to its room of origin. Rather, the smoke and hot gases flow into adjacent rooms, corridors or stairwells, igniting the content of these compartments. The manner in which a fire propagates through a multi-enclosure structure is very dependent on the geometry, materials and contents of the building. It also depends on the state of the doors and windows, whether they are open or closed, and on whether the windows break or other structural components, such as walls, floors, ceiling and roof, are breached by the fire. Of course external conditions, such as wind flow patterns and brands, also have great influence on the progression of the fire, and therefore, on the heat release rate (HRR) accorded to the structure.

Zone models, which take advantage of physics-based mathematical submodels of these processes, are considerably simpler than the field models, usually resulting in a mathematical formulation consisting of nonlinear ordinary differential equations in time and complex algebraic relations between dependent variables. The model CFAST [11] is a recent example from NIST of this class of models

Field models require considerably more data and computational resources and can provide substantially more detail about fire behaviour than zone models: as noted above, zone models are more global and less detailed in their descriptions of fire growth and spread than field models. Therefore, for fires in buildings, field models, in principle, should be able to provide finer detail over smaller regions, for given computational resources, while zone models should be able to compute fire behaviour while providing less detail over many more burning rooms.

In this spirit for outdoor fires, assuming we need more detail than current operational models, but less than current field models, a simple model is proposed for wind-driven fire spread in heterogeneous, coupled fuel systems, namely ones with continuous fuel beds and also discrete fuel elements, on a scale of interest for WUI fires. While the model is modest and has significant limitations, it represents an attempt to carry out a physics-based coupling dynamically. The model can be viewed as analogous to zone models described above, and it is simple enough that it might be coupled into current operational models, such as BehavePlus [4] and FARSITE [5] in a usable fashion.

In many ways, this model can be regarded as a dynamical extension of the model of Baum and McCaffrey [12]. In that paper, the authors derived a dynamically consistent solution to the mass and energy equations for an outdoor plume. This mathematically sophisticated solution is very useful because, as discussed below, it provides both scaling relations and detailed velocity profiles for this fundamental configuration. Baum and McCaffrey [12] then applied their plume model to the study of mass fires. Since this model is dynamically consistent, it describes the global flow field induced by the object burning with the prescribed HRR. That is, it describes the induced flow both near the burning object and at distance from it. Dold *et al.* [13] have labelled this property as non-local effects. Therefore, for more than one burning object, one can superimpose the individual flow fields to obtain the nonlocal wind pattern determined by these heat sources.

The plume model was also used by Ohlemiller and Corley [14] to estimate the thermally-induced winds generated during large-scale mass-fire experiments carried out by Forestry Canada. The estimated winds were found to be consistent with the measured winds during the experiments. Similarly, Trelles and Pagni [15] used this model to estimate the winds generated by multiple burning houses at various times during the Oakland Hills fire of 1991. These predicted winds were then compared with measured wind data at the same times, and it was found that significant wind changes occurred, consistent with the model predictions, at nearly the same times. Specifically during the Oakland Hills fire, over a 15 minute interval, from 11:45 am to 12 noon on 20 October 1991, the number of houses burning was found to increase from 38 to 259, producing dramatic changes in the winds consistent with the increased burning.

The model proposed here has the advantage that, while very simple, it is physics based without the computationally and data intensive requirements associated with the field models. Furthermore, the model is dynamical, not static; it accounts for dynamical fire front evolution with time.

In Section 3, data on heat content, burning rate and heat release rates (HRR) for Australian grass fires and theoretical estimates of these quantities for structural fires are presented. An attempt is made to introduce rate processes in a way that will be useful for our proposed mathematical model. Then, in Section 4, a simple mathematical model is presented for the propagation of a grass fire driven by the wind field from an ambient wind plus one or more burning houses. The idea is to utilize the wind field determined from the Baum–McCaffrey [12] plume to describe the wind field of a single burning structure. That model, which is summarized in the Section 4.1, requires the specification of a heat release rate (HRR) for the structure and provides both characteristic length- and velocity-scales, as well as the detailed normalized entrainment velocity as a function of distance from the centre of the structure. For purposes of this study, the peak HRR has been used for each burning structure. The scaling of the effects on the fire front due to structure size, and, for multiple structures, structure spacing and number of houses, is discussed in Section 4.2. In Section 4.3 and in the appendix in more detail, a Lagrangian description of the spread of an initial line fire in grass for a general wind field is presented. Features of this model are illustrated by examples in Section 5. Finally, a summary and conclusions are presented in Section 6.

3. Heat release rates of grass and structure fires

Rehm *et al.* [16] reviewed the literature on the potential energy content of various wildland fuels and compared these numbers with the potential energy content of structures. The purpose of that comparison was to estimate the density of structures required for the potential energy content to be equal to that of a particular wildland fuel. That work emphasized the importance of the potential energy content of the structures as part of the overall energy available, without regard for the dynamical processes required to ignite the fuels, sustain and propagate the fire, and with no estimate of the duration and completeness of the combustion processes.

This section extends that previous work by considering time-dependent processes for grass and structural fuels. Burning time-scales, heat release rates (HRR) and propagation speeds for grass fires are compared with estimates of burning times, HRR and entrainment winds produced by ventilation-controlled structure fires.

3.1. Grass fires

Mell *et al.* [8] have compared data obtained from Australian grass-fire experiments with modelling results obtained by using the Wildland Fire Dynamics Simulator (WFDS). The experiments

Table 1. Data for testing WFDS model presented by Mell *et al.* [8] from Australian grass-fire experiments carried out by CSIRO and reported by Cheney *et al.* [18, 19].

Experiment	Fire-line intensity (MW/m)	Rate of spread (ROS)(m/s)
Case F19	5.5	1.4
Case CO64	4.4	1.2

were carried out by CSIRO and were reported and analysed by Cheney *et al.* [17–19]. The simulations were carried out with WFDS, a variant of the Fire Dynamics Simulator (FDS) code developed at NIST by McGrattan [7] and based on the techniques of computational fluid dynamics (CFD). This study is perhaps the most complete comparison between results from a modern mathematical/computational model and burn data for grasses.

Quantities from these grass-fire papers utilized in the present study are the rate of spread (ROS) of the fire-line, the fire-line intensity and the total heat release rate (HRR). The relationship below, presented in the paper of Cheney *et al.* [19], determines the ROS, r_w , in m/s for an Australian grass fire as a function of the ambient wind speed, V_a also in m/s, the effective width W of the fire-line in metres and the dead fuel moisture percentage M_f :

$$r_w = 0.165(1 + 3.24 V_a)\exp[(-0.859 - 2.04 V_a)/W] \cdot \exp(-0.108 M_f)[\text{m/s}] \quad (1)$$

The dimension of r_w is m/s and is shown in square brackets. For simplicity in the examples below, I have utilized the limit of very small moisture content and very long fire-lines, so that $r_w \approx 0.165(1 + 3.24 V_a)$. For the study of Mell *et al.*, two example burns, designated as F19 and CO64, were examined in detail, and are listed in Table 1. The values given in the table have a precision of only two significant figures, which reflects their uncertainty. Although other numbers may be transcribed below to the precision given in their sources, a precision of two significant figures is probably all that can be trusted in most cases.

For comparison, Table 2 is reproduced from [16]. This table consists of data originally presented by Albini [17], with some of the data converted to SI units that are more convenient for the comparison. For example, the spread rate data in column 2 was given originally by Albini in miles per hour; it is converted to metres per second in column 3. The ROS and the fire-line intensity allow one to determine the total HRR and a burn duration for a specified length of fire-line.

Table 2. Types of wildfires, rate of spread (ROS) and intensities as reported by Albini [17]. Also shown are fuel energy density implied by these values.

Types of wildfire	Spread rate (mi/h)	ROS (m/s)	Intensity (MW/m)	Fuel energy density (GJ/hectare)
Ground fire	0.00003	0.0000083	0.00001	12
Surface fires				
Marginal conditions	0.01	0.003	1	3.7
‘Good’ conditions	10	2.77	10	36
Grass fires	20	5.54	1	1.8
Debris fires	1	0.277	10	370
Crown fires	3	0.833	10	121

3.2. Structure fires

An estimate of the energy release rate during a house fire in the 1991 Oakland Hills fire was reported by Trelles [21] and by Trelles and Pagni [15]. According to these estimates, a house burns at a peak rate of 45 MW for 1 h (yielding about 160 GJ), and then dies down over another 6 h period. The die-down of the fire is approximated as two steps, one 10 MW for 3 h and the last as 5 MW for 3 more h. The total burn time is 7 h, and the total energy released by the house is 324 GJ. If, as assumed also, there is brush around each house which releases another 5 MW for one hour, then an additional 18 GJ of energy will be released. If the house is assumed to be 15 m by 15 m by 5 m, then we estimate the total potential fuel loading per unit area to be of order 1.4 GJ/m^2 , the peak HRR per unit area to be of order 0.2 MW/m^2 . For comparison, oil yields a heat release rate per unit area of approximately 2 MW/m^2 [6, 22].

Confirmation of this estimate for the magnitude of the peak HRR for a burning structure can be found in the chapter on compartment fires in the book on fire behaviour by Quintiere [23]. Here, Quintiere describes the stages of a fire in a compartment and estimates the peak heating rates possible during the latter stages of a compartment fire, when the fire is fully developed and ventilation limited. Ventilation limited merely means that the burning rate is restricted by the amount of air entering the enclosure, and this amount is determined by the size of the vents in the enclosure. During this period, the flow in and around the enclosure is driven by buoyancy, which is generated by the burning taking place both inside and outside the compartment.

In one example, Quintiere estimates a total HRR of 9 MW for a compartment in which the fuel load is taken to be proportional to the floor area, that in this case is 12 m^2 . He points out that, this peak HRR could increase to over 60 MW if the fuel was proportional not only to the floor area, but to the whole inside area of the compartment. Such a lined compartment might be much more characteristic of a cabin in the woods, for example, for which the wall and ceiling were constructed of wood. Furthermore, a multi-room structure, with a fuel loading of the more modest type, producing 9 MW for each room, could also easily exceed the roughly 50 MW peak HRR estimated by Trelles and Pagni [15]. Therefore, based on compartment fire analysis, it seems very plausible that structure fires could have peak HRR reaching several times this estimate of 50 MW, and the duration of these peak HRR would be measured in tens of minutes or hours.

These estimates say nothing about the fact that the roof of the structure might develop a hole or even collapse under prolonged vigorous burning. In that case, the fire might then resemble more a burning crib than an enclosure fire. They also say nothing about the effects of winds on peak heat release rate or burn duration. It seems likely that winds would increase the peak HRR and reduce the burn duration, but the magnitude of these changes is not known. For our purposes here, the estimates above will be used without trying to assess these other effects.

4. A simple model for WUI ground-fire spread

Models that address WUI fire spread must necessarily be complex because of the heterogeneity of the fuel. As noted earlier, the usual conceptual models for the interaction of a wildfire with structures regard the structures as isolated in the middle of wildland fuels and implies a density of houses that is so low that the burning of these houses has no effect on the progression of the wildfire.

In reality, often there are many structures in addition to the wildfire itself that can contribute to the overall fire spread. For example, in Figure 1 a photograph by John Gibbons of the San Diego Union-Tribune is shown of the 2003 Cedar Fire about to invade the Scripps Ranch residential community. If the structures in this figure were to be ignited by brands (or other means), then the fire front would be invading a community with burning structures.



Figure 1. Photograph of the Cedar Fire approaching the Scripps Ranch residential community.

Here a model for the wind-driven spread of a ground fire in a WUI setting is presented. While very simple, it does offer some insight and quantitative estimates of one important growth mechanism, ground-fire spread by a combination of ambient wind and the wind generated by burning houses. Ignition between fuel elements, i.e. grass to structure, structure to grass or structure to structure envisioned in this model takes place by direct flame impingement of the relatively small grass flames, by brands or embers, which can either ignite structures directly, or start spot fires in the grass that can ignite a structure ahead of the fire front, or possibly by direct house-to-house fire spread. Such inter-fuel ignition is reasonable. An example of such fire spread is discussed in a USDA report by Murphy *et al.* [24], which describes a post-fire assessment of the Angora Fire related to fuel treatment methods.

Assume an array of uniformly spaced, identical houses for $y \geq 0$ (see the schematic diagram in Figure 2), and a constant ambient wind V_a in the positive y -direction blowing a grass fire front across the houses from below.

In the remainder of this section, a mathematical formulation of this conceptual model is presented.

4.1. Plume model of Baum and McCaffrey

The paper by Baum and McCaffrey [12] is the starting point for the analysis reported here. In that paper there is a fundamental analysis of the structure of a plume and its associated flow field produced by a pool fire in a quiescent atmosphere. An empirical correlation for centreline temperature and velocity was determined from the compilation of data obtained from a large number of pool-fire experiments carried out by many investigators over a wide range of pool-fire diameters. Based on the buoyant, inviscid equations of motion and this correlation, the analysis obtains the scaling relations for the characteristic length- and velocity-scales for a pool-fire plume. Furthermore, a detailed velocity profile is determined from a solution to these equations.

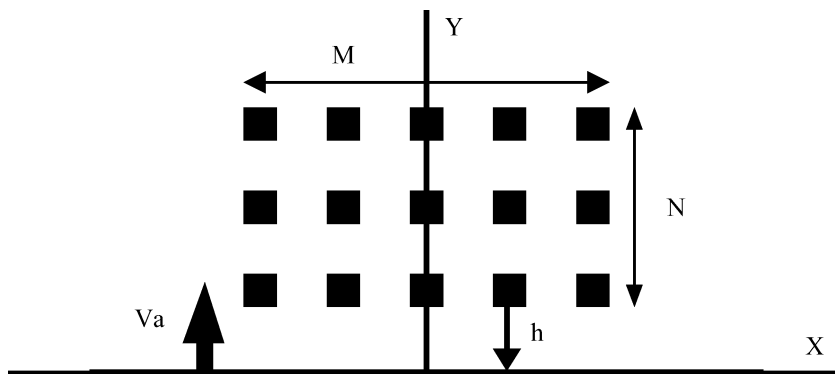


Figure 2. A schematic of an array of uniformly spaced, identical houses with a constant ambient wind V_a blowing a fire front (red) across the houses.

Our analysis utilizes this plume model to describe the flow field generated by a single burning house and to estimate the effects of this flow field on the progression of a ground fire. The import of the analysis, I believe, is that it demonstrates with a simple physics-based model and an inexpensive computational scheme that a house, once ignited, becomes part of the fuel system and affects fire-line progression. It also allows us to investigate the changes in the fire-line spread as various parameters are changed, such as the number and location of burning structures.

The model of Baum and McCaffrey [12] is for a single buoyancy-driven plume in an inviscid, quiescent fluid of density ρ_0 , temperature T_0 and pressure P_0 at ground level. The magnitude of the heat release rate of the source is designated as Q_0 , and the specific heat of the air is denoted as C_p . The model starts with the equations for mass, momentum and energy, assuming axial symmetry. The velocity field is then decomposed by a fundamental theorem of vector analysis into two components, one specifying the divergence and the other the curl. The divergence of the velocity results from thermal expansion of the gas, and the curl is the vorticity, and these components can be related to the plume centreline temperature and velocity correlations. From this analysis, the following scaling arises:

$$D^* = \left(\frac{Q_0}{\rho_0 C_p T_0 \sqrt{g}} \right)^{2/5}$$

$$V^* = \sqrt{g D^*} \quad (2)$$

where D^* = length-scale [m], Q_0 = heat source [W], ρ_0 = ambient density [kg/m^3], C_p = specific heat at constant pressure [J/kg], T_0 = ambient temperature [K], g = acceleration of gravity [m/s^2] and V^* = velocity-scale [m/s].

Finally, a detailed solution for the velocity field, which is valid both inside and outside the plume, was found by Baum and McCaffrey. This velocity field at ground level is shown in Figure 3.

4.2. Scaling relations

The scaling relations obtained from the plume analysis of Baum and McCaffrey can be used to estimate the importance of burning structures on wind-blown fire spread in the WUI. In

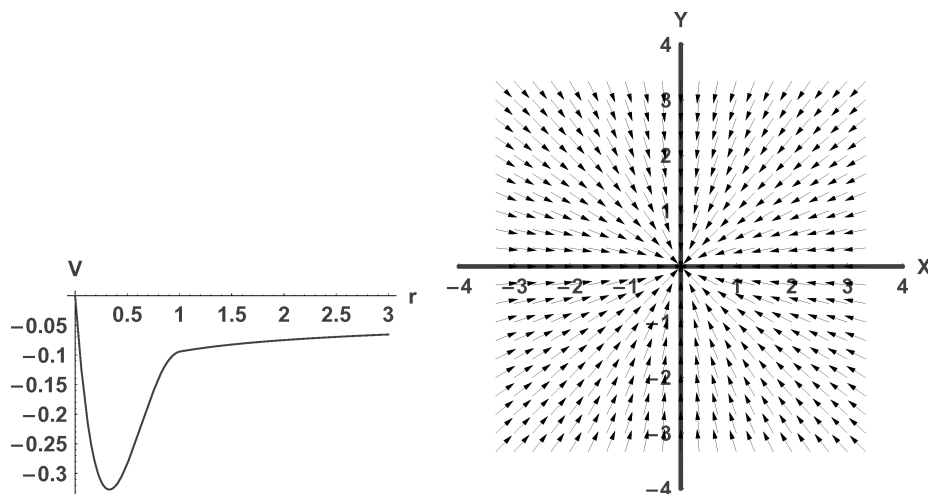


Figure 3. Left: Normalized entrainment velocity induced by a structure fire at ground level versus normalized radial distance from the centre of the fire. Right: Entrainment velocity vectors at ground level induced by a burning structure.

Tables 3 and 4, characteristic quantities are presented, followed by the definitions and units in square brackets, first for structure fires (Table 3), then for wildland fires (Table 4).

These characteristic quantities, coupled with the model described above, lead to several interesting conclusions. We consider two cases, that of a fire front propagating past a single burning structure and that of a fire front propagating past an array of burning structures. This latter case is shown schematically in the Figure 2, where the front is initially a straight line along the x -axis, blown by an ambient wind toward the array. The array is considered to be rectangular with M structures in the x -direction and N structures in the y -direction, with the single house being the special case of $M = N = 1$.

First, consider the ratio of the entrainment velocity V^* to the rate of spread U of the fire front in the absence of wind as a function of the heat release rate (HRR) for a single burning structure. This ratio is plotted at the left of Figure 4. Note, that this ratio is about 10 for even the rather modest value for the HRR of 20 MW, and increases with HRR to about 35 at the large value of 2000 MW for the HRR. This relatively large ratio can be considered in part to result from the

Table 3. Characteristic scaling quantities for cases of structure fires.

Structure Fire	Fire size (small)	Fire size (moderate)	Fire size (large)	Fire size (very large)
Q_0 [MW]	25	50	100	500
D^* [m]	7.5	12	19	55
V^* [m/s]	8.6	11	14	23
τ_s [s]	4×3600	14400	14400	14400
E_s [GJ]	360	720	1440	7200

Q_0 = heat release per unit time for the structure [MW].

D^* = length-scale of the plume (characterized by Q_0) [m].

V^* = velocity-scale of the plume (characterized by Q_0) [m/s].

τ_s = burning time for the house [s].

E_s = potential energy of the structure [GJ].

Table 4. Characteristic scaling quantities for cases of wildland fires.

Parameter	Grass (low)	Grass (medium)	Grass (high)	Trees
Structure density [No./acre]	4	4	1	0.25
L [m]	32	64	128	32
I [MW/m]	5	5	5	10
U [m/s]	1	1	1	1
τ [s]	36	36	36	36
m_f [kg/m ²]	0.06	0.06	0.06	0.6
h [MJ/kg]	20	20	20	20
e [MJ/m ²]	1.2	1.2	1.2	12

L = length between structures (the spatial period) [m].
 I = the fire-line intensity [MW/m].
 U = the rate of spread (ROS) of the fire front [m/s].
 τ = the passage time for the fire front [s].
 m_f = the mass of wildland fuel per unit area [kg/m²].
 h = burnable energy per unit mass of wildland fuel [MJ/kg].
 (Note: 1 acre = 4047 m², and 1 hectare = 10 000 m².)

fact that the fuel in the structure is concentrated, or discrete, whereas that in the wildland fuel is uniformly distributed over the area.

Next, for an array of regularly spaced burning structures, separated by a distance $2L$ in each direction, the y -component of the total entrainment velocity at a position x, y is

$$v_{\text{total}}(x, y, L, V^*, D^*) = \sum_{j=0}^N \sum_{i=-l}^l V^* v \left(\frac{\sqrt{(x - 2iL)^2 + (y - 2jL)^2}}{D^*} \right) \times \frac{(y - 2jL)}{\sqrt{(x - 2iL)^2 + (y - 2jL)^2}} \tag{3}$$

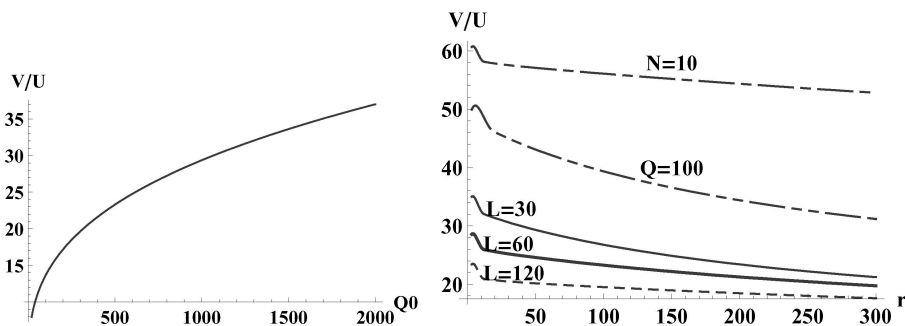


Figure 4. Left: The ratio of the characteristic entrainment velocity to the rate of spread (ROS) of the fire front as a function of the heat release rate (HRR) of a burning structure in megawatts (MW). Right: The ratio of the characteristic entrainment velocity to the rate of spread (ROS) of the fire front as a function of the distance of the fire front from a square array of $N \times N$ houses each separated by a length L and burning with a HRR Q_0 . The base case is labelled $L = 60$ and has $L = 60$ m, $N = 5$, and $Q_0 = 50$ MW.

where we have used $I \equiv (M - 1)/2$ in all cases presented. Equation (3) yields a value for the y -component of the characteristic entrainment velocity as a function of several parameters. Plots of this expression are shown at the right in Figure 4. The plot shows the enhancement of the entrainment velocity over the fire front ROS for multiple structures as a function of the distance $r = y$ from the centre of the middle structure in the first row. Other parameters are the structure separation $2L$, the HRR Q_0 of each structure, and the total number of structures M in the x -direction by N in the y -direction. This plot shows the collective effect of the array of burning houses. The base case in this set of plots is for $L = 60$ m, $M = N = 5$ houses and $Q_0 = 50$ MW; it is the curve labelled as $L = 60$. Naturally, as the number of houses, M by N , increases, the enhancement increases. Also, as Q_0 , for each house increases, the enhancement increases. As the spacing, $2L$, between houses increases, the entrainment decreases. The spacing $2L$ can also be interpreted as the housing density. As the housing density increases, the spacing decreases; this point is discussed in Section 5.

The cluster of three curves labelled by L show what happens when the base case L is doubled or halved, whereas the other two curves show what happens when $M = N$ is doubled or when Q is doubled. A somewhat surprising feature of these plots is the magnitude of the enhancement. The magnitude of the collective effect is a result of the fact that the entrainment velocity for each plume drops off with distance from the the plume centre as one over the distance to the one-third power. However, all of these effects (and the relative surprises) can be inferred from the analysis of the plume model given by Baum and McCaffrey [12].

4.3. Fire-front propagation

For the spread of a wildfire, it is usual to consider a fire front of arbitrary shape advancing into unburned fuel. Behind the front, the fuel is assumed to be burned, and the front is taken to be thin relative to other dimensions of the problem. The model for the front propagation can then be formulated mathematically in two related but different descriptions. One is the so-called Lagrangian description and the other is an Eulerian description [25, 26]. In the former formulation, the advance of each Lagrangian particle on the front is related to the empirically determined rate of spread (ROS) of a fire at the locally determined wind speed. It is the most straightforward description and requires following only a one-dimensional, time-dependent array of these Lagrangian particles. The latter formulates the problem as a two-dimensional, time-dependent, convection-diffusion partial differential equation, for which the fire front at any time is a 2D curve representing a constant value of a dependent variable of the problem. According to Sethian [25], this formulation offers some advantages for following the front progression. However, a distinct disadvantage of this formulation is that it requires solution of a partial differential equation (PDE) in two spatial dimensions and time.

In the description of the spread of wildfires, it is often assumed that the fire-front propagation takes place according to Huygen's principle [5, 26–28]. Huygen's principle states that the location of a propagating front after a small increment of time can be found from its earlier location by calculating the envelope of the wavelets emitted from all points along the earlier front. Huygen's principle has been widely used in a variety of applications; it was originally developed to explain and calculate optical wave front growth, but has been applied to a other areas as well [25].

Richards [27] used an approximate form of Huygen's principle to determine the growth of a wildfire front. It was implemented into the operational wildfire prediction code, FARSITE [5]. This conceptual model has also been used to describe the spread of fronts in combustion as well as in other applications; see for example [25, 29, 30].

For our purposes, we consider the Lagrangian description, and take as the governing equations, the two ordinary differential equations (ODEs) describing the propagation of each Lagrangian

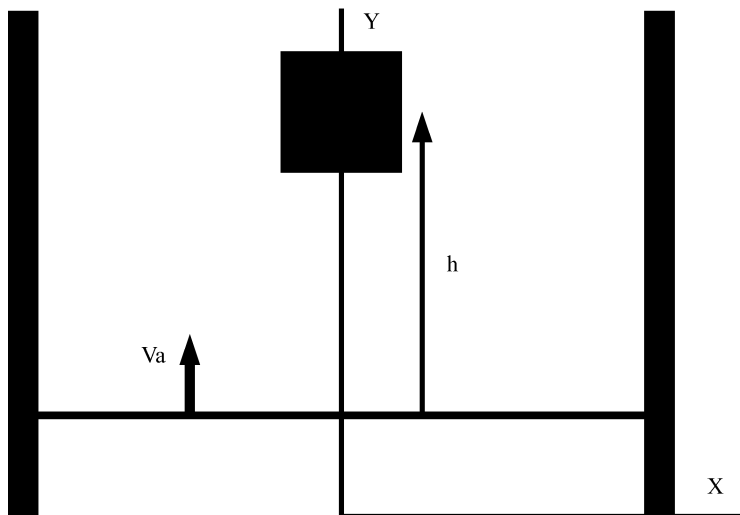


Figure 5. The initial fire-line (red), the structure, axes and the periodic boundary conditions at $x = L$ and $x = -L$.

element in the x, y -plane.

$$\begin{aligned} \frac{dx}{dt} &= U_n n_x \\ \frac{dy}{dt} &= U_n n_y \end{aligned} \tag{4}$$

where x, y is the location of the Lagrangian element on the fire front, U_n is the normal component of the spread-rate vector of the fire front at the location (x, y) , and n_x, n_y are the components of the unit normal to the fire front directed toward the unburnt fuel. The fire front curve at any specified time t is described by the vector function $(x(s, t), y(s, t))$, where s is a parameter determining the distance along the curve.

At each point, the fire front is advanced in the direction normal to the front at a speed determined by the local ROS for the fire. This ROS, in turn, depends on the wind speed at that location. One might regard this procedure as a method-of-characteristics calculation. For computational purposes, the fire front is discretized and then moved incrementally to its new location as described below. We start with an approximation to the normal ROS, and then numerically solve the governing equations. We use the Method of Lines (MOL) and a centred difference scheme for the spatial discretization of the fire-line. The discussion below describes a wind-blown grass fire using Equation (1) to relate the ROS of the fire to the local wind speed.

For a fire front exposed to the velocity field generated by a burning structure of HRR Q_0 , the characteristic length- and velocity-scales are D^* and V^* as discussed above. Let \vec{r}' denote the vector distance from the centre of the structure to the element of the fire front. The velocity at this point will be $v(r') = V^*v(r'/D^*)$, where $v(r'/D^*)$ is the dimensionless velocity and D^* is the length-scale defined above, and the dimensionless vector distance, \vec{r} , is $\vec{r} = \vec{r}'/D^*$. In addition, we assume that there is a uniform (in space and time) ambient wind \vec{V}_a , which is added vectorially to the entrainment velocity.

Let the fire-line initially be a straight line along the x -axis, running between $-L$ and L . We divide this interval into a discrete set of nodes and use the method of lines (MOL) to solve the equations for the motion of these nodes. Details of the mathematical equations for following the fire front are presented in the appendix, and solutions are given and discussed in the next section.

We have developed and solved the simplest example that illustrates the effects of burning structures on fire front propagation. We consider an initially straight fire front parallel to the x -axis and propagating in the y -direction. See the schematic diagram in Figure 5.

5. Results and discussion

This simple wind-blown model for WUI fire front propagation depends on several parameters. At this time, only a fraction of these effects have been examined, and then only for a limited set of values for the parameters. In the results presented here, the problem has been specialized to examine fire-front propagation of an initially straight fire-line of length $2L$ propagating past a structure. This formulation has permitted a good understanding of the physical processes governing the propagation in a computationally efficient and robust fashion.

As discussed above, the scaling relations presented earlier are very important. They demonstrate the effects, for example, of housing density on ground-fire propagation. The spatial period $2L$ between structures determines the housing density:

$$2L = \sqrt{\frac{A}{n}} \quad (5)$$

where n is the number of houses and A is the area considered. It is easy to think of A being an acre ($= 4047 \text{ m}^2$) and n as the number of houses on that acre, since, in a typical suburban area, a house lot is about $1/4$ acre. Therefore, $n = 4$, and $2L = 32 \text{ m}$. The top curve of the three curves labelled by L in the right plot in Figure 4 is for $L = 30 \text{ m}$ (or approximately one house per quarter acre – a typical suburban neighbourhood). The second of the three plots ($L = 60 \text{ m}$) is for a housing density of one house per 4 acres while the third plot ($L = 120 \text{ m}$) is for a housing density of 1 house per 16 acres. Recall that these three plots in Figure 4 are for an array of 25 ($M = N = 5$) houses with $Q_0 = 50 \text{ MW}$ per house. The remaining two plots show what happens to the base case $L = 60 \text{ m}$ when each parameter is doubled, $M = N = 10$ or $Q_0 = 100 \text{ MW}$ with the other parameters for the base case remaining the same.

Two sets of results for the detailed computations described above are shown in each of Figures 6 and 7. Figure 6 shows plots for a single house while Figure 7 shows plots for the centre house in a single line ($N = 1$) of five houses. In the left plot of Figure 6, the fire front progression is shown for a structure burning at 200 MW intensity with an ambient wind speed of 2 m/s blowing toward the top of the diagram. The structure is 12 m on a side, the fire front is shown every 25 s starting as a straight line 30 m below the centre of the burning structure and the length of the initial fire-line is $2L = 60 \text{ m}$. In the plot on the right, the conditions are the same except that the fire front starts initially 10 m behind the burning structure; i.e. it is assumed that the fire front has passed the house before it ignites and becomes fully involved.

The model for the entrainment effects of a single burning house on the fire front assumes there are no neighbouring burning structures. For the case of a ‘line of houses’ (see Figure 7), the fire front location at various times is shown for the centre house of a line of five burning structures,

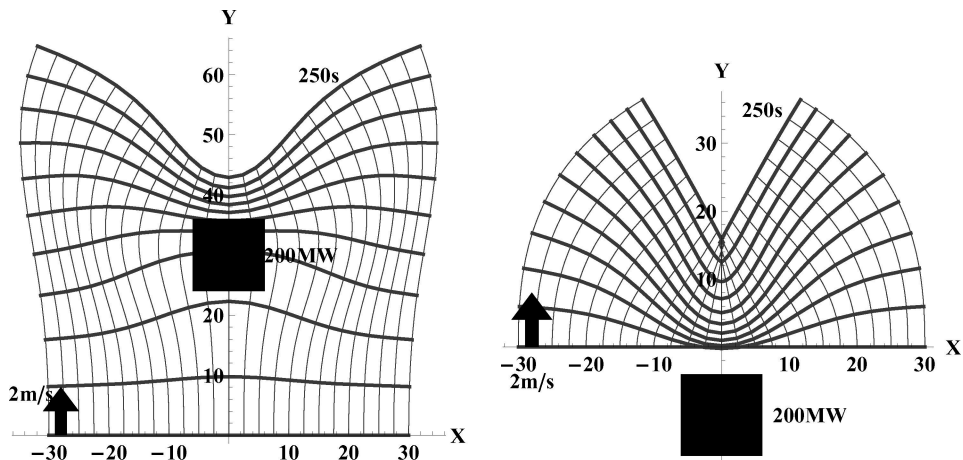


Figure 6. The fire front at several equal time intervals for a burning structure with an ambient wind of 2 m/s, a 200 MW fire and $L = 30$ m. Left: House is burning before arrival of fire front. Right: House ignites after passage of fire front.

and includes the entrainment wind generated by the house shown and its four neighbouring houses on both sides.

An advantage of this model is that it is very fast and resolves the fire front with a minimum number of nodes, even when several burning structures are assumed involved. For other formulations, resolving the fire front when several burning structures are involved, can be much more computationally intensive and much less robust. The examples shown in this section have all been computed in real time or less in a computational development environment. Therefore, this methodology for calculating WUI fire spread could potentially be incorporated into current operational models.

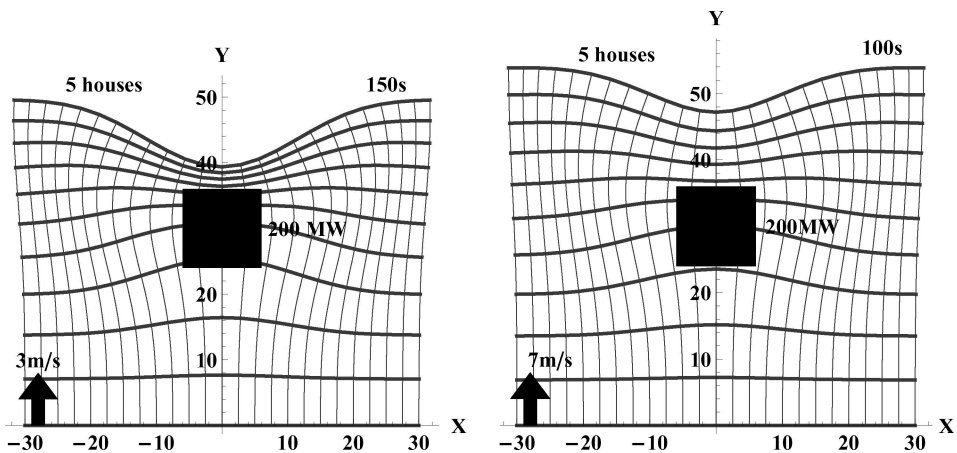


Figure 7. The fire front at several equal time intervals near the centre structure of a line of five burning structures. Left: Ambient wind of 3 m/s. Right: Ambient velocity of 7 m/s.

In each case in Figure 7, the fire front initially is a straight line 30 m below the centreline of the five burning structures. In the left plot, there is an ambient wind of 3 m/s while in the right plot there is a 7 m/s ambient wind. In each plot, the time interval between fire front locations is the same; in the left plot it is 15 s and in the right 10 s. For all cases shown in Figures 6 and 7, the fire front is accelerated as it approaches the structure and is retarded after it passes. However, for the line of houses, the entrainment velocity is enhanced by the accumulative effect of the row of burning structures, thereby accelerating the fire front more as it approaches the burning houses and retarding it more after passing the houses.

Note that the primary influence of the entrainment winds from burning houses on the overall propagation of a grass-fire front is determined by the scaling relations given in Equation (3) and illustrated in Figure 4. These relations show that the fuel system for WUI fires must include structures as well as vegetation, and that the progression of a grass-fire front (and probably other vegetation fire fronts also) can be altered substantially when a large number of structures are burning. The plots in Figures 6 and 7 show examples of detailed fire-front propagation changes due to burning structures and also show that these changes can be tracked in a computationally inexpensive and robust fashion. Even in such a simple model, several parameters determine the details of the fire-front propagation, and only a few of these variations have been presented here.

6. Summary and conclusions

There are several ideas upon which the proposed model are based. These are:

1. The time-scale associated with burning grass and burning individual trees is measured in tens of seconds in contrast with the time-scale for burning structures, which is measured in tens of minutes to hours. Therefore, the coupling between the natural fuel burning and the structure fuel burning is loose. For example, burning houses are shown to influence grass fire propagation, but, excluding ignition (about which little has been said here), it is not clear how grass fires influence the burning of houses. Furthermore, because of the disparity in time-scales, it will be difficult to utilize a field model such as FDS to compute multiple burning houses and vegetative (WUI) fires over large areas in any detail due to constraints on computational resources. For example, the cases shown here have all been computed in real time or less in a computational development environment, orders of magnitude faster than current field models. Therefore, using field models for operational guidance on large-area WUI fires in the near term is unlikely.
2. The heat release rate of a structure fire determines the strength of its plume and defines a characteristic length-scale and a characteristic velocity-scale for the entrainment of the plume. The peak HRR has been used in all examples to illustrate the effects. This model requires that the plume stand upright, and, therefore, that the ambient wind be less than the characteristic plume velocity.
3. The ground level entrainment velocity resulting from the plume model of Baum and McCaffrey decays with radial distance r from the plume as $r^{-1/3}$ at large distances. This slow decay implies that the entrainment has significant influence over large distances, and the mass-fire study of Baum and McCaffrey illustrates this fact. It shows up here in the large enhancement factor caused by a single burning structure and also in the even larger enhancement factor arising from multiple burning structures. Furthermore, the magnitude of the enhancement factor for multiple burning structures is found to increase significantly as the housing density increases, or as the separation distance between (burning) houses decreases, and also as the HRR for each structure increases.

4. The influence of the entrainment winds from burning houses on the overall propagation of a grass-fire front is demonstrated by the scaling relations given in Equation (3) and illustrated in Figure 4. These relations show that the fuel system for WUI fires must include structures as well as vegetation, and that the progression of a grass-fire front (and probably other vegetation fire fronts also) can be altered substantially when a large number of structures are burning. The plots in Figures 6 and 7 show examples of detailed fire-front propagation changes due to burning structures and also show that these changes can be tracked in a computationally inexpensive and robust fashion. Even in such a simple model, several parameters determine the details of the fire-front propagation, and only a few of these variations have been presented here.
5. The selection of the present model for a grass-fire front propagating past burning structures provides a simple, convenient example of a WUI fire that allows direct comparison between the line-fire effects and the structure-fire effects; see Tables 3 and 4 for some direct comparisons. This comparison is much more natural than earlier models attempted. The strength of a front is measured by the line-fire intensity, its rate of spread and the energy density of wildland fuel. From these quantities and the spatial length, all of the necessary parameters can be obtained for comparison with the corresponding quantities obtained from a periodically placed set of structures.

Acknowledgements

This research was supported in part by NIST Contract Number SB1341-05-W-1003; I wish to thank Anthony Hamins who served as the Contract Monitor. Several colleagues have contributed through discussions and constructive suggestions. Thanks to NIST colleagues Alex Maranghides, Sam Manzello, Anthony Hamins, Ruddy Mell, Kevin McGrattan and Howard Baum and to Simo Hostikka of VTT Building and Transport, Finland, and Dave Evans of the SFPE.

Appendix

In this appendix, equations are presented for determining the fire front propagation in the presence of burning structures. The governing equations are the ordinary differential equations (ODEs) describing the propagation of an element of the fire front in the horizontal plane:

$$\frac{d\vec{R}}{dt} = (\vec{U} \cdot \vec{n})\vec{n} \quad (6)$$

The equations are given in vector form $\vec{R} = x\vec{i}_x + y\vec{i}_y$, where \vec{i}_x, \vec{i}_y are unit vectors in the x - and y -directions. $\vec{U} = U_x\vec{i}_x + U_y\vec{i}_y$ is the rate of spread (ROS) vector of the fire front at the location (x, y) , and n_x, n_y are the components of the unit normal to the fire front directed toward the unburnt fuel.

At each point, the fire front is advanced in the direction normal to the front at a speed determined by the local ROS for the fire. This ROS, in turn, can depend on several variables including the wind speed at that location. Let $\vec{V}_T = V_{Tx}\vec{i}_x + V_{Ty}\vec{i}_y$ be the wind velocity at a specified height. Assume that the linear relation given in Equation (1) between the ROS and the local wind velocity is valid for the components of the ROS and the local wind normal to the fire front:

$$U_n = \text{ROS}_0(1 + c_f V_n)$$

where $U_n = \vec{U} \cdot \vec{n}$ and $V_n = \vec{V}_T \cdot \vec{n}$ with $\text{ROS}_0 = 0.165$ [m/s] and $c_f = 3.24$. Then

$$\frac{d\vec{R}}{dt} = \text{ROS}_0(1 + c_f \vec{V}_T \cdot \vec{n})\vec{n}$$

If the fire front curve at any specified time t is described by the vector function $(x(s, t), y(s, t))$, where s is a parameter specifying the curve, then, the unit normal is

$$\begin{aligned} n_x &= \frac{-\partial y/\partial s}{\sqrt{(\partial x/\partial s)^2 + (\partial y/\partial s)^2}} \\ n_y &= \frac{\partial x/\partial s}{\sqrt{(\partial x/\partial s)^2 + (\partial y/\partial s)^2}} \end{aligned} \tag{7}$$

For a fire front exposed to the velocity field generated by a burning structure of HRR Q_0 , the characteristic length- and velocity-scales are D^* and V^* as given in Equation (2). Let \vec{r}' denote the vector distance from the centre of the structure to the element of the fire front. The entrainment velocity at ground level at this point will be $V_e(r) = V^*v(r'/D^*)$, where $v(r'/D^*)$ is the dimensionless velocity, $\vec{r} = \vec{r}'/D^*$ is the dimensionless vector distance from the burning structure to the element of the fire front and where $r' = |\vec{r}'|$ and $r = |\vec{r}|$.

The detailed solution for the dimensionless velocity function at ground level, $v(r)$ was obtained analytically by Baum and McCaffrey in terms of special functions. For computational purposes, however, this solution was replaced in the example calculations presented here by the functional form given below, which closely approximates the analytical solution.

$$\begin{aligned} v(r) &= ar + br^2/2 + cr^3/3 + dr^4/4 \quad 0 \leq r \leq r_0; \\ v(r) &= ar_0 + br_0^2/2 + cr_0^3/3 + dr_0^4/4 - \frac{f_0(r - r_1)^2}{2(r_1 - r_0)} + \frac{f_1(r - r_0)^2}{2(r_1 - r_0)} + \frac{f_0(r_1 - r_0)}{2} \\ &\quad r_0 \leq r \leq r_1; \\ v(r) &= \left[ar_0 + br_0^2/2 + cr_0^3/3 + dr_0^4/4 + \frac{(f_0 + f_1)}{2(r_1 - r_0)} \right] \left(\frac{r_1}{r} \right)^{(1/3)} \quad r_1 \leq r; \end{aligned}$$

where $r_0 = 0.8$, $r_1 = 1.0$, $f_0 = 0.407199$, $f_1 = 0.045029$, $a = -2.39441$, $b = 11.2283$, $c = -13.6154$, $d = 4.9468$.

For a single burning structure at $(x = h, y = H)$, the induced entrainment velocity components at any point (x, y) are

$$\begin{aligned} V_x &= \frac{x - h}{\sqrt{(x - h)^2 + (y - H)^2}} V^*v(\sqrt{(x - h)^2 + (y - H)^2}/D^*) \\ V_y &= \frac{y - H}{\sqrt{(x - h)^2 + (y - H)^2}} V^*v(\sqrt{(x - h)^2 + (y - H)^2}/D^*) \end{aligned} \tag{8}$$

We also assume that there is a uniform (in space and time) ambient wind \vec{V}_a , at the specified height which is added vectorially to the entrainment velocity, $\vec{V}_T = \vec{V}_e + \vec{V}_a$. Let the ambient wind have components $(V_a \sin \theta_a, V_a \cos \theta_a)$, where V_a is the ambient wind speed and θ_a is the angle of the ambient wind relative to north. Then the total wind velocity components at (x, y) are

$$\begin{aligned} V_{Tx} &= V_a \sin \theta_a + \frac{(x - h)}{\sqrt{(x - h)^2 + (y - H)^2}} V^*v(\sqrt{(x - h)^2 + (y - H)^2}/D^*) \\ V_{Ty} &= V_a \cos \theta_a + \frac{y - H}{\sqrt{(x - h)^2 + (y - H)^2}} V^*v(\sqrt{(x - h)^2 + (y - H)^2}/D^*) \end{aligned} \tag{9}$$

We note that this formulation can be extended easily to multiple burning structures by vectorially summing the entrainment contributions from each of the structures and the ambient velocity to give the total velocity locally.

For computational purposes, the fire front is discretized and then moved incrementally to its new location as described below. We start with an approximation to the normal ROS, and then numerically solve

the governing equations. We use the Method of Lines (MOL) and a centred difference scheme for the spatial discretization at all interior nodes of the fire front. For the end nodes, we use a one-sided difference scheme with the neighbouring interior node.

Let the fire-line initially be a straight line along the x -axis, running between $-L$ and L . We divide this interval into $2I$ panels each of length δ , where $\delta = 1/I$. The nodes for the numerical solution are therefore placed at $x_i = i\delta$, where the index i varies between $-I$ and I . We use a centred difference discretization to approximate the unit normal at each node along the fire-line:

$$\begin{aligned}n_{x,i} &= \frac{-(y_{i+1} - y_{i-1})}{\sqrt{(x_{i+1} - x_{i-1})^2 + (y_{i+1} - y_{i-1})^2}} \\n_{y,i} &= \frac{(x_{i+1} - x_{i-1})}{\sqrt{(x_{i+1} - x_{i-1})^2 + (y_{i+1} - y_{i-1})^2}}\end{aligned}\quad (10)$$

We take a one-sided difference at end nodes with the neighbouring interior node.

After discretization, we can write the ordinary differential equations (ODEs) in the interior of the fire front, for $i = -I + 1, -I + 2, \dots, I - 2, I - 1$, as

$$\begin{aligned}\frac{dx_i}{dt} &= U_{x,i} \cdot \frac{-(y_{i+1} - y_{i-1})}{\sqrt{(x_{i+1} - x_{i-1})^2 + (y_{i+1} - y_{i-1})^2}} \\ \frac{dy_i}{dt} &= U_{y,i} \cdot \frac{(x_{i+1} - x_{i-1})}{\sqrt{(x_{i+1} - x_{i-1})^2 + (y_{i+1} - y_{i-1})^2}}\end{aligned}\quad (11)$$

Separately we must write the equations for the end nodes. At the left,

$$\begin{aligned}\frac{dx_{-I}}{dt} &= U_{x,-I} \cdot \frac{-(y_{-I+1} - y_{-I})}{\sqrt{(x_{-I+1} - x_{-I})^2 + (y_{-I+1} - y_{-I})^2}} \\ \frac{dy_{-I}}{dt} &= U_{y,-I} \cdot \frac{(x_{-I+1} - x_{-I})}{\sqrt{(x_{-I+1} - x_{-I})^2 + (y_{-I+1} - y_{-I})^2}}\end{aligned}\quad (12)$$

Similarly, at the right

$$\begin{aligned}\frac{dx_I}{dt} &= U_{x,I} \cdot \frac{-(y_I - y_{I-1})}{\sqrt{(x_I - x_{I-1})^2 + (y_I - y_{I-1})^2}} \\ \frac{dy_I}{dt} &= U_{y,I} \cdot \frac{(x_I - x_{I-1})}{\sqrt{(x_I - x_{I-1})^2 + (y_I - y_{I-1})^2}}\end{aligned}\quad (13)$$

As stated above, the initial conditions for these equations are $y_i(0) = 0$ and $x_i(0) = \delta * i$ for $-I \leq i \leq I$.

References

- [1] F. Albini, *An overview of research on wildland fire*, In *Proceedings of the Fifth International Symposium on Fire Safety Science*, International Association for Fire Safety Science (IAFSS), Melbourne, Australia, 3-7 March 1997, pp. 59-74.
- [2] R.C. Rothmel, *A Mathematical Model for Predicting Fire Spread in Wildland Fuels*, USDA Forest Service Research Paper INT-115, 1972.
- [3] R.C. Rothmel, *How to Predict the Spread and Intensity of Forest and Range Fires*, USDA Forest Service Technical Report INT-143, 1983.

- [4] D. Carlton, P. Andrews and C. Bevins *BehavePlus Fire Modeling System: User's Guide; Quick Start Tutorial*, USDA Forest Service, Rocky Mountain Research Station, Systems for Environmental Management, 2004. Online Help development: <http://fire.org/>
- [5] M.A. Finney, *FARSITE: Fire Area Simulator – Model Development and Evaluation*, United States Department of Agriculture, US Forest Service, Rocky Mountain Research Station, Research Paper RMRS-RP-4, March 1998, Revised 2004. <http://fire.org/>
- [6] K.B. McGrattan, H.R. Baum and R.G. Rehm, *Numerical simulation of smoke plumes from large oil fires*, *Atmos. Environ.* 30 (1996), pp. 4125–4136.
- [7] K.B. McGrattan, *Fire Dynamics Simulator (Version 4)*, Technical Reference Guide, NISTIR Special Publication 1018, National Institute of Standards and Technology, Gaithersburg, MD, 2004. <http://fire.nist.gov/bfrlpubs/>
- [8] W. Mell, M.A. Jenkins, J. Gould and P. Cheney, *A physics based approach to modeling grassland fires*, *Internat. J. Wildland Fire* 16 (2007), pp. 1–22. <http://www2.bfrl.nist.gov/userpages/wmell/public.html>
- [9] R.R. Linn, *Transport Model for Prediction of Wildfire Behavior*, Los Alamos National Laboratory Scientific Report LA13334-T, 1997.
- [10] G.P. Forney and K.B. McGrattan, *User's Guide for Smokeview Version 4 – A Tool for Visualizing Fire Dynamics Simulation Data*, NIST Special Publication 1017, 2004.
- [11] W.W. Jones, R.D. Peacock, G.P. Forney and P.A. Reneke, *CFAST – Consolidated Model of Fire Growth and Smoke Transport (Version 6) Technical Reference Guide*, NIST Special Publication 1030, 2004. <http://fire.nist.gov/bfrlpubs/>
- [12] H.R. Baum and B. McCaffrey, *Fire induced flow field – Theory and experiment*, in *Fire Safety Science – Proceedings of the Second International Symposium*, Hemisphere Publishing, Newport, Australia, 1989, pp. 129–148.
- [13] J. Dold, A. Zinoviev and R. Weber, *Nonlocal flow effects in bushfire spread rates*, In *Proceedings of the Fifth International Conference on Forest Fire Research* D.X. Viegas, ed., 2006.
- [14] T. Ohlemiller and D. Corley, *Heat release rate and induced wind field in a large scale fire*, *Combust. Sci. Technol.* 94 (1994), pp. 315–330.
- [15] J. Trelles and P.J. Pagni, *Fire-induced winds in the 20 October 1991 Oakland hills fire*, in *Fire Safety Science – Proceedings of the Fifth International Symposium*, Melbourne, Australia, Y. Hasemi, ed., 1997, pp. 911–922.
- [16] R.G. Rehm, A. Hamins, H.R. Baum, K.B. McGrattan and D.D. Evans, *Community-scale fire spread*, in *Proceedings of the California 2001 Wildfire Conference: 10 Years After the 1991 East Bay Hills Fire*, 10–12 October 2001, K.S. Blonski, M.E. Morales, and T.J. Morales, eds., Oakland California Technical Report 35.01.462. Richmond CA; University of California Forest Products Laboratory, pp. 126–139; Also, NISTIR 6891, July, 2002.
- [17] F. Albin, *Wildland fires*, *American Scientist*, Nov.–Dec. (1984), pp. 590–597.
- [18] N.P. Cheney, J.S. Gould and W.R. Catchpole, *The influence of fuel, weather and fire shape variables on fire spread in grasslands*, *Internat. J. Wildland Fire* 3 (1993), pp. 31–44.
- [19] N.P. Cheney and J.S. Gould, *Fire growth in grassland fuels*, *Internat. J. Wildland Fire* 5 (1995), pp. 237–247.
- [20] N.P. Cheney, J.S. Gould and W.R. Catchpole, *Prediction of fire spread in grasslands*, *Internat. J. Wildland Fire* 8 (1998), pp. 1–13.
- [21] J. Trelles, *Mass fire modeling of the 20 October 1991 Oakland Hills fire*, PhD Thesis in Mechanical Engineering, University of California at Berkeley, 1995.
- [22] H.R. Baum, K.B. McGrattan and R.G. Rehm, *Simulation of smoke plumes from large oil fires*, in *Twenty-Fifth Symposium (International) on Combustion*, The Combustion Institute 25 (1994), pp. 1463–1469.
- [23] J. Quintiere, *Principles of Fire Behavior*, Delmar Publishers, Albany, NY, 1997.
- [24] K. Murphy, T. Rich and T. Sexton, *An Assessment of Fuel Treatment Effects on Fire Behavior; Suppression Effectiveness, and Structure Ignition on the Angora Fire*, USDA Report R5-TP-025, 2007.
- [25] J.A. Sethian, *Level Set Methods and Fast Marching Methods, Evolving Interfaces in Computational Geometry, Fluid Mechanics, Computer Vision, and Materials Science*, Cambridge University Press, Cambridge, 1999.
- [26] F.E. Fendell and M.F. Wolff, *Wind-aided fire spread*, in *Forest Fires, Behavior and Ecological Effects* E.A. Johnson and K. Miyanishi, eds., Academic Press, San Diego, 2001, Chapter 6, pp. 171–223.
- [27] G.D. Richards, *An elliptical growth model of forest fire fronts and its numerical solution*, *Internat. J. Numer. Meth. Engng* 30 (1990), pp. 1163–1179.

- [28] G.D. Richards, *The properties of elliptical wildfire growth for time dependent fuel and weather conditions*, Combust. Sci. Technol. 92 (1992), pp. 145–171.
- [29] A.R. Kerstein, W.T. Ashurst and F.A. Williams, *Field equations for interface propagation in an unsteady homogeneous flow field*, Phys. Rev. A 37 (1988), pp. 2728–2731.
- [30] R.C. Aldredge, *The scalar-field front propagation equation and its applications*, in *Modeling in Combustion Science; Proceedings of the US–Japan Seminar*, Kapaa, Kauai, Hawaii, 24–29 July 1994, J. Buckmaster and T. Takeno, eds., Lecture Notes in Physics, Springer-Verlag, Berlin, 1995, pp. 23–35.